Thyroid Research

RESEARCH

Open Access

Celastrol promotes apoptotic cell death in thyroid cancer cells through a caspases-dependent pathway

Ruoyi Yang[1,2†], Jie Yao[3†], Hong Ma[1], Chunyan Shui[2], Teng Li[1], Sicheng Zhang[2*] and Chao Li[1,2*]

Abstract

Background Celastrol, a naturally occurring bioactive compound, has demonstrated potential in treating inflammation, obesity, and tumors, particularly in colorectal, gastric, and breast cancers. However, its therapeutic effects on thyroid cancer (TC), which have poor clinical outcomes, remain unclear. This study aimed to investigate Celastrol's potential in treating thyroid cancer using cell lines.

Methods The viability and proliferation of thyroid cancer cells treated with or without Celastrol were analyzed by CCK-8 and colony formation assay. The state of thyroid cancer cells treated with or without Celastrol were observed by microscopy. Further evidence from flow cytometry and TUNEL staining demonstrated the induction of apoptotic processes in thyroid cancer cells. The expression of PARP1, Caspase-3, Bax, BCL2 in thyroid cancer cells after indicated treatment was analyzed by Western blot and Caspase-3 expression in thyroid cancer cells after 12 and 24 h of Celastrol treatment was detected by immunofuorescence assay. Anaplastic thyroid cancer growth-limiting of Celastrol was evaluated in nude mice.

Results Celastrol induction promoted apoptotic in TC cells, increased the expression of PARP1, Bax and Caspase-3 and reduces expression of BCL2 by Western Blot. The expression of Caspase-3 was increased by immunofluorescence, which indicating that Celastrol may serve as an adjuvant therapeutic agent for thyroid cancer treatment by inducing apoptosis through the caspase-3 pathway. Celastrol treatment of mice implanted with anaplastic thyroid cancer cells also inhibited tumor growth, associated with reduced Ki-67 and increased Caspase-3.

Conclusions Celastrol promotes apoptotic cell death in thyroid carcinoma cells by the Caspase-3 pathway.

Highlights

Key findings • Celastrol has been found to promote apoptotic cell death in thyroid cancer cells, offering potential for the development of new anti-cancer drugs.

[†]Ruoyi Yang and Jie Yao contributed equally to this work and are considered co-first authors.

*Correspondence:
Sicheng Zhang
zhangsicheng@scszlyy.org.cn
Chao Li
lichao@scszlyy.org.cn
Full list of author information is available at the end of the article

What is known and what is new? • The anti-cancer effect of Celastrol is known. The ability of Celastrol to promote apoptosis in thyroid cancer does our manuscript adds.

What is the implication, and what should change now? • Utilizing Celastrol as a therapeutic drug for thyroid cancer may provide a new treatment option, particularly for patients who are unresponsive to conventional approaches. This discovery holds promise for improving survival rates and quality of life for thyroid cancer patients.

Keywords Celastrol, Papillary thyroid carcinoma, Medullary thyroid carcinoma, Anaplastic thyroid cancer, Apoptotic, Caspase-3

Introduction

Thyroid cancer (TC) is the most common malignancy in the endocrine system, with its incidence steadily increasing [1]. It can be categorized into papillary thyroid carcinoma (PTC), follicular thyroid carcinoma (FTC), medullary thyroid carcinoma (MTC), and anaplastic thyroid cancer (ATC) based on pathological characteristics [2, 3]. PTC, accounting for 80% of cases, typically carries a favorable prognosis with a 10-year survival rate of approximately 90% [4]. However, PTC is prone to recurrence and metastasis, especially in aggressive forms, leading to resistance to treatment and potential fatality [5–7]. MTC, a rare form of thyroid cancer, represents 3–5% of cases [8]. Approximately 75% of MTC cases in patients are non-hereditary, while the remaining 25% are hereditary [9]. Although its incidence is low, MTC has a relatively high mortality rate due to early metastasis [10, 11], with approximately 35% of MTC patients experiencing neck metastasis and approximately 13% showing distant metastasis [12]. ATC is among the most aggressive and lethal malignancies, predominantly affecting individuals aged 65 to 70, with a median overall survival of 3.16 months and a near 100% mortality rate [13, 14]. Despite comprising only 1–1.5% of thyroid cancers, ATC contributes to over half of the annual thyroid cancer-related deaths [15]. Current treatment options for poor-prognosis PTC, MTC, and ATC involve surgical resection and molecular targeted therapy to improve symptoms and survival rates. However, targeted therapy can lead to adverse reactions such as gastrointestinal issues and hypertension. In contrast, traditional Chinese medicine, such as Celastrol, may offer a potentially safer alternative.

Celastrol is a pentacyclic triterpenoid monomer isolated from the Thunder God Vine, a traditional Chinese herbal medicine [16, 17]. It was the first active compound to be isolated from Thunder God Vine. Celastrol has shown great potential in the areas of anti-inflammation, obesity treatment, and anti-tumor therapy [18–20]. Studies have demonstrated that Celastrol, as a novel anticancer agent, can induce cancer-specific cell death while having minimal cytotoxicity in normal cells [21, 22]. However, few studies have investigated the potential anticancer effects of Celastrol on PTC, MTC and ATC cells. Therefore, in this study, we aimed to investigate the effects of Celastrol on PTC, MTC and ATC cells, providing new insights into the anti-thyroid cancer mechanisms of Celastrol.

Methods

Cell culture

The human cell lines MDA-T32, KTC-1 (PTC) were obtained from the research group in the early stages, while TT (MTC) was generously provided by Prof. Zheng from Zhejiang Provincial People's Hospital, and OCUT-2C (ATC) was kindly provided by Prof. Luo from West China Hospital. PTC cells were cultured in RPMI-1640 Medium, MTC was cultured in Ham's F-12 K Medium, and ATC was cultured in DMEM. The culture media were supplemented with 1% v/v Penicillin–Streptomycin Solution and 10% v/v FBS. Cells were maintained at 37 °C in a humidified atmosphere with 5% CO2. Celastrol obtained from MCE, was dissolved in 1% DMSO.

Cell viability assay

The cells were seeded into 96-well plates (5000 cells/well) with 3 replicates for each group at each time point. After 24 h incubation, 200 μL of medium containing 10% cell counting kit-8 (CCK-8) (KeyGEN Biotech, Nanjing, China) was added to each well. The CCK-8 assay was applied to detect the cell viability following the manufacturer's protocols. This experiment was performed in triplicate.

Colony formation assay

Thyroid cancer cell lines (600 cells/well) were seeded into 6-well plates and treated with different concentration of Celastrol. After incubated at 37 °C for 10 d, the cells were washed with PBS, fixed with 4% paraformaldehyde solution and stained with 1% crystal violet for 15 min. The colony numbers were counted by a light microscope. This experiment was performed in triplicate.

Flow cytometry

Thyroid cancer cells were divided into a control group and a Celastrol treatment group. The MDA-T32, KTC-1,

TT, and OCUT-2C cell lines (1×10^4 cells/well) were seeded in 12-well plates and incubated for 24 h. Cell apoptosis was assessed using the Annexin V/PI staining kit (MULTISCIENCES, Hangzhou, China) following the manufacturer's instructions. The cells were collected, detached, and washed twice with PBS before resuspending in 200 μL of binding buffer. Compensation adjustment was performed using a blank tube, an Annexin V single-staining tube, and a PI single-staining tube. Annexin V and PI solutions were added to the control and Celastrol treatment groups, respectively, and incubated at room temperature for 5 min. Flow cytometry was conducted to determine the percentage of apoptotic cells. This experiment was performed in triplicate.

Western blot analysis

Thyroid cancer cells were divided into a control group and a Celastrol treatment group. The MDA-T32, KTC-1, TT, and OCUT-2C cell lines (60×10^4 cells/well) were seeded in 6-well plates and incubated for 24 h. The cells were lysed with RIPA buffer, and the supernatant was collected after centrifugation. Protein concentration was determined using a BSA kit, and samples were prepared for analysis. Samples were separated by 10% SDS-PAGE and transferred onto PVDF membranes. The membranes were blocked with TBS buffer containing 0.01% Tween 20 and 5% skim milk at room temperature for 1 h. After three washes, the membranes were incubated overnight at 4 °C with a diluted primary antibody (1:2000). Following three washes, the membranes were incubated with a diluted horseradish peroxidase-conjugated secondary antibody (1:5000) at room temperature for 1 h. After three washes, immunoreactive bands were detected using an enhanced chemiluminescence kit (Bio-Rad). Protein quantification was analyzed using ImageJ software and normalized to the respective controls.

TUNEL staining

The thyroid cancer cells were divided into control groups, Celastrol treatment groups, and positive groups. After 24 h of treatment, the cells were fixed with 4% paraformaldehyde at 37 °C for 30 min and permeabilized with 1% Triton X-100 for 5 min. The positive samples were treated with a prepared DNase I reaction solution at 37 °C for 30 min. TUNEL solution was added to all groups and incubated at 37 °C in the dark for 1 h. TRITC red fluorescence was added and incubated in a wet box at 37 °C in the dark for 30 min. The cell nuclei were counterstained with 0.1 μg/mL DAPI at room temperature for 5 min. Three fields were randomly selected for observation using a laser confocal fluorescence microscope. ImageJ software was used to analyze the TUNEL-positive cells and total cells. The red fluorescence indicated TUNEL-positive cells.

Immunofluorescence assay

After 12,24 h of treatment with Celastrol, the thyroid cancer cells in the control group and the Celastrol treatment group were fixed with 4% paraformaldehyde at 37 °C for 60 min and permeabilized with 0.1% Triton X-100 for 10 min. After blocking with 5% bovine serum for 30 min at room temperature, the cells were incubated overnight at 4 °C with a primary antibody against Caspase-3. Fluorescence was generated by incubating with Alexa Fluor® 594-labeled goat anti-rabbit IgG at 37 °C for 1 h. DAPI was used to counterstain the cell nuclei. Fluorescence images were captured using a laser confocal fluorescence microscope, and ImageJ was employed to quantify the fluorescence intensity.

In vivo xenograft model

Female nude mice (4–6 weeks old) were obtained from the Laboratory Animal Center and housed under standard conditions. Mice were randomly divided into three experimental groups: control, Celastrol 1 mg/kg, and Celastrol 2 mg/kg. OCUT-2C cells were injected subcutaneously into the left flank of all mice at 2×10^6 cells in 100 μL PBS. After day 10 of cell injection, treatment of mice was initiated. A Treatment commenced on day 10 when tumors reached a volume of 50–100 mm^3.Treatments included Celastrol at 1 or 2 mg/kg every other day by intraperitoneal injections. Control mice received PBS vehicle. Tumor volumes were determined by measuring length (l) and width (w) and calculating volume ($V=0.5\times l\times w^2$) at the indicated time points. Treatments were maintained for 14 days. Mice were sacrificed, and tumor tissues were removed, weighed, and photographed. Samples were used for histology and proteins level determination.

Tissue immunohistochemistry

Xenograft tumors from nude mice were fixed in 4% paraformaldehyde for 24 h and embedded in paraffin. Paraffin microtomy was used to create sections, which were then baked overnight at 65 °C. The sections underwent rehydration with graded alcohols, followed by treatment with citrate buffer (pH = 6.0) and hydrogen peroxide. After blocking with 5% BSA for 1 h, the sections were incubated overnight at 4 °C with primary antibodies (Ki-67, Caspase-3). Subsequently, they were incubated with an HRP-conjugated secondary antibody and stained with DAB.

Statistical analysis

SPSS 18.0 software (IBM, San Francisco, CA, USA) was applied to conduct the statistical analyses. For the comparison of two groups, Student's t test was used. For the comparison of more than two groups, one-way analysis of variance was used. $^{*}p<0.05$, $^{**}p<0.01$, $^{***}p<0.001$, $^{****}p<0.0001$.

Results

Celastrol induced cell death in thyroid cancer cells

In this study, we aimed to investigate the effects of Celastrol on four human thyroid cancer cell lines: KTC-1 and MDA-T32 (PTC), TT (MTC), and OCUT-2C (ATC). Cell viability was assessed using a CCK-8 assay, and the results showed that Celastrol significantly suppressed the viability of all four cell lines in a dose- and time-dependent manner. Notably, the TT cell line required a higher concentration of Celastrol compared to the other cell lines for similar levels of suppression (Fig. 1A-D). Colony formation assays revealed reduced growth in all four cell lines with increasing Celastrol concentrations. However, due to the characteristics of TT cells, they exhibited poor cluster formation in the assay. Nevertheless, TT cell growth decreased with higher Celastrol concentrations (Fig. 1E). Microscopic examination revealed extensive cell death in all four cell lines, indicating the induction of cell death by Celastrol (Fig. 1F). Overall, our findings demonstrate that Celastrol inhibits thyroid cancer cell viability and growth, and promotes cell death, highlighting its potential as a therapeutic agent for thyroid cancer treatment.

Celastrol induced apoptosis in thyroid cancer cells

In our study, we used Annexin V/PI staining flow cytometry to evaluate the effects of Celastrol on cells. Our analysis demonstrated that Celastrol treatment significantly induced apoptosis in all four cell lines (Fig. 2A). We also performed Western blot analysis to examine the expression levels of PARP1, Caspase-3, Bax, and BCL2 proteins in the control and Celastrol-treated groups. Our results showed that Celastrol treatment increased the expression levels of PARP1, Caspase3, and Bax proteins, while decreasing the expression level of BCL2 protein in all four cell lines (Fig. 2B). These findings support the pro-apoptotic effects of Celastrol on the cell lines and suggest that Celastrol induces apoptosis by modulating these key apoptosis-related proteins. Additionally, we employed the TUNEL method to assess apoptosis levels in the control and Celastrol groups. Our results showed a higher number of TUNEL-positive apoptotic cells in the Celastrol group compared to the control group (Fig. 2C). These findings demonstrate a notable increase in the rate of apoptosis in the cell lines following Celastrol administration.

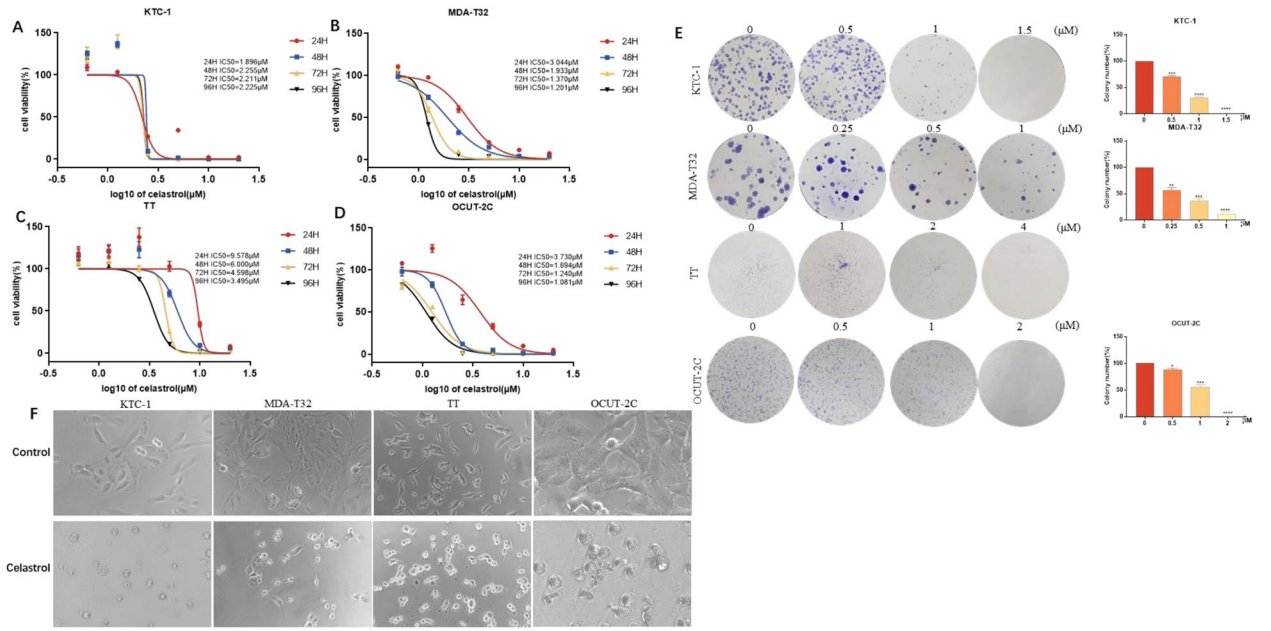

Fig. 1 Celastrol induces death in thyroid cancer cells. **A**-**D** Effect of Celastrol on the viability of human Thyroid cancer cells. Cells were challenged with increasing concentrations of Celastrol for 24h,48h,72h or 96h and cell viability was measured by CCK-8. IC50 values in different cell lines (KTC-1 and MDA-T32 (PTC), TT (MTC), and OCUT-2C (ATC)) are shown; **E** Colony formation assays: cells were treated with various doses of Celastrol for 24h and then allowed to grow for 10 days in fresh culture medium. Colonies were visualized by crystal purple staining; **F** Morphological alterations induced by Celastrol treatment

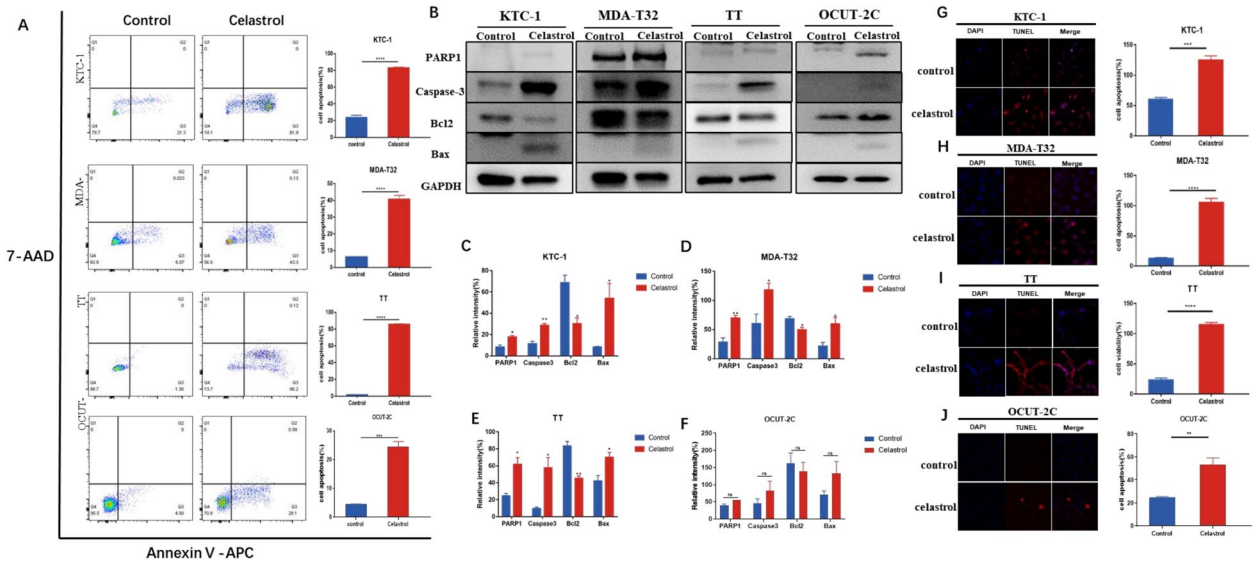

Fig. 2 Celastrol induces apoptosis in thyroid cancer cells. **A** Apoptotic cell frequencies treated without or with Celastrol for 24 h were determined by annexin V/PI assays; **B**-**F** KTC-1, MDA-T32, TT and OCUT-2C were treated with Celastrol for 24 h; The expression of cleaved-PARP 1, Caspase-3, BCL2 and Bax; **G**-**J** Changes of TUNEL-positive cell rate among Celastrol and control group for 24 h

Celastrol treatment induced apoptosis through Caspase-3 pathways

Immunofluorescence staining was employed to visualize apoptotic cells via the Caspase-3 pathway. Our results showed that the number of apoptotic cells in the Celastrol-treated group was significantly increased compared with the control group, and the apoptotic cells showed typical morphological changes, such as cell shrinkage, chromatin condensation, and fragmentation. Furthermore, the expression of Caspase-3 was significantly upregulated in MDA-T32 (Fig. 3A) [12h:t = 7.702, $p < 0.01$; 24h:t = 11.02, $p < 0.001$], KTC-1 (Fig. 3B) [12h:t = 8.492, $p < 0.01$; 24h:t = 17.11, $p < 0.0001$], TT (Fig. 3C) [12h:t = 12.33, $p < 0.001$; 24h:t = 17.34, $p < 0.0001$], and OCUT-2c (Fig. 3D) [12h:t = 4.781, $p < 0.01$; 24h:t = 6.043, $p < 0.001$] cells treated with celastrol for 12h and 24h, compared to the control group.

Celastrol suppressed tumor growth of anaplastic thyroid carcinoma cells in vivo

To establish our in vivo cultivation study, we injected OCUT-2C cells into nude mice and initiated Celastrol treatment at a dose of 1 or 2 mg/kg. Follow-up on day 14 revealed that Celastrol treatment reduced the growth of anaplastic thyroid carcinoma (Fig. 4A). While the 1 mg/kg dose was effective in inhibiting tumor growth, Celastrol at a dose of 2 mg/kg completely halted tumor growth (Fig. 4B). Analysis of harvested tumor specimens demonstrated that immunohistochemical staining indicated reduced levels of Ki-67 in Celastrol-treated nude mice. Celastrol also elevated the levels of Caspase-3, confirming increased apoptosis of tumor cells in vivo, consistent with our in vitro findings, and reducing the immunoreactivity of Ki-67 in tumor cells (Fig. 4C-E).

Discussion

Thyroid cancer, particularly PTC, is the most common neoplasm in the endocrine system. Surgery is the primary treatment, but metastatic PTC can have a poor prognosis. MTC is rare but highly lethal, often accompanied by metastases. MTC is influenced by both somatic cells carrying the RET oncogene and germline inheritance [23], with RET serving as a key therapeutic target [24]. However, resistance to tyrosine kinase inhibitors (TKIs) is a challenge. Therefore, the development of new drugs targeting alternative targets has also become a crucial aspect of MTC treatment [25]. ATC is a highly difficult tumor with a short diagnosis-to-treatment window and high resistance rates. Promising treatment options for ATC include Aurora kinase inhibitors, which have shown an 86% reduction in tumor volume in mouse models. Other potentially promising treatment modalities include gene therapy using oncolytic viruses, novel targeted inhibitors, immunotherapy, and combination therapies. Identifying therapeutic targets and conducting related drug research is crucial to enhance the survival rate and quality of life for ATC patients [15]. Celastrol, a bioactive compound extracted from Thunder God Vine, has been extensively studied for its therapeutic effects on obesity and inflammation [26]. In fact, Celastrol has great

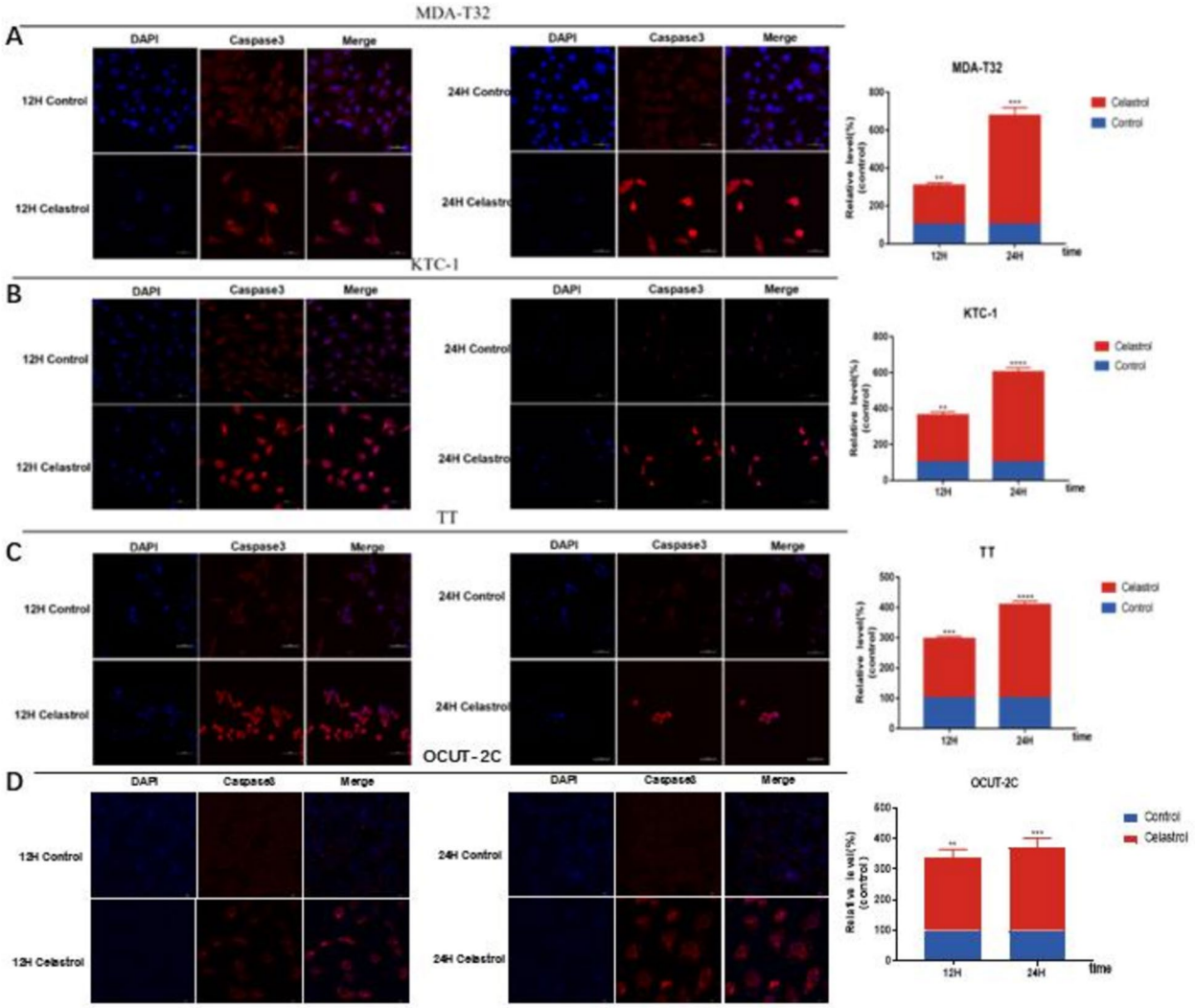

Fig. 3 Celastrol treatment induces apoptosis through Caspase-3 pathways. Immunofluorescence analysis of Caspase-3 expression in MDA-T32 (**A**), KTC-1 (**B**), TT (**C**), and OCUT-2c (**D**) cells treated with celastrol for 12h and 24h. Positive fluorescence intensity of immunofluorescent Caspase-3 antibody was observed and quantified at both time points. Representative images were captured for each cell type

potential in anti-tumor treatment, as evidenced by studies such as Heng et al. [27] demonstrating that Celastrol inhibits colon cancer by targeting peroxidase 1 in in vitro and in vivo experiments, Yang et al. showing that Celastrol promotes apoptosis in neuroblastoma cells through the caspase pathway in in vitro experiments [28], and Celastrol exerting anti-tumor effects in non-small cell lung cancer by inhibiting ROS accumulation [29].

The purpose of this study was to investigate the potential of Celastrol to treat poorly differentiated PTC and MTC. We first verified that Celastrol induced apoptosis of PTC, MTC and ATC cells in a concentration- and time-dependent manner using a cell viability test. We also observed reduced cell numbers, condensed nuclei, and ruptured cytoplasm under the microscope after 24 h of Celastrol treatment. In the colony formation experiment, we observed that the cell clusters of PTC cells decreased with increasing Celastrol concentration. However, due to the growth characteristics of MTC cells, which mainly grow as single cells, have low cell adhesion and lack the ability to form cell aggregates, TT cells were difficult to form cell clusters in the colony formation experiment. But we also clearly observed that TT cells also gradually decreased with increasing Celastrol concentration. To further verify whether Celastrol really induces apoptosis of MTC, PTC and ATC cells we performed flow cytometry, protein immunoblot assay and TUNEL assay. The results showed that Celastrol induced early apoptosis of

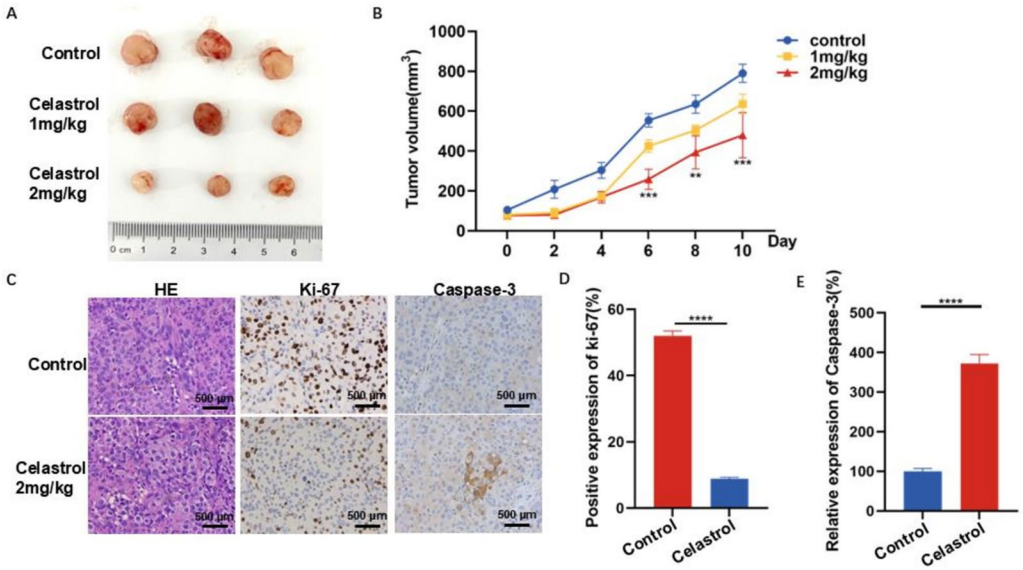

Fig. 4 Celastrol suppressed tumor growth of ATC cells in vivo. **A** Original photo of tumor in tumor bearing mice under Celastrol treatment; **B** Tumor growth curve of tumor bearing mice under Celastrol treatment; **C** Performing HE and IHC staining on the transplant tumor (40X). **D** The IHC analysis revealed a significantly lower Ki-67 positivity rate in the Celastrol-treated group compared to the control group; **D**) The IHC analysis showed a significant increase in the cytoplasmic staining percentage of Caspase-3 in the tumor samples from the Celastrol-treated group compared to the control group

thyroid cancer cells. Immunofluorescence experiment also confirmed that Celastrol indeed induced apoptosis of MTC, PTC and ATC cells. Caspase-3 pathway plays an irreplaceable role in cell apoptosis. We found by immunofluorescence experiment that Celastrol induced cell apoptosis through Caspase-3 pathway. Subsequently, we conducted an in vivo study using nude mice, where undifferentiated thyroid carcinoma cells (OCUT-2C) were injected into the mice. Tumor growth was monitored, and when the tumors reached 50 mm3, alternate-day treatment with Celastrol was initiated. On the 14th day of treatment, it was observed that the tumor tissue in the Celastrol 2 mg/kg treatment group exhibited significant shrinkage compared to the control group. These findings corresponded with the results obtained from in vitro experiments.

Immunohistochemical staining of the nude mouse tumor tissue revealed a decrease in Ki-67 and an increase in Caspase-3 in the Celastrol 2 mg/kg treatment group compared to the control group, indicating the efficacy of Celastrol at this dosage in the in vivo experimental setting.

This experiment proves through various in vitro experiments that Celastrol can induce apoptosis of thyroid cancer cells and only verifies that it is induced through Caspase-3 pathway. Furthermore, the in vivo experiments on nude mice provided additional evidence that tumor tissue exhibited noticeable shrinkage in both macroscopic observation and measurement when treated with Celastrol at a concentration of 2 mg/kg on an alternate-day dosing schedule, compared to the control group. Additionally, the presence of Caspase-3 induction pathway was confirmed in the tumor tissue. But does not completely verify how Celastrol induces apoptosis through Caspase-3 pathway or in what way. Further in-depth research is still needed. At present, traditional Chinese medicine ingredients are widely studied in clinics, but there are also side effects on the human body. Therefore, These alone are not enough to translate to the clinic and further verification of relevant toxic side effects is still needed.

In conclusion, we have demonstrated that Celastrol can induce apoptosis in thyroid cancer cells through the activation of the Caspase-3 pathway. These findings suggest that Celastrol may be a potential new anti-thyroid cancer drug. This discovery provides a new avenue for the development of effective therapies for thyroid cancer. Further research can explore the mechanism of action of Celastrol in thyroid cancer treatment, as well as evaluate its feasibility and safety for clinical use.

Conclusions

The present study indicated that Celastrol promotes apoptotic cell death in PTC, MTC and ATC cells by the Caspase-3 pathway. Moreover, in the in vivo experiments on nude mice with ATC, Celastrol was also effective

in reducing tumor size. However, the present study is on the basis of cell experiment and superficial animal experiments. Further comprehensive research and clinical investigations are needed to uncover the underlying mechanisms of Celastrol in treating thyroid cancer.

Acknowledgements
The authors gratefully acknowledge financial support from the Sichuan Province Regional innovation cooperation project (2024YFHZ0215); the State Key Laboratory of Oral Diseases (SKLOD) Open Fund(Sichuan University)(SKLOD2024OF02); the Key Project of the Sichuan Provincial Health Commission's Clinical Research Program (24LCYJZD06).

Authors' contributions
Ruoyi Yang: Investigation, Validation, Visualization, Writing-original draft. Jie Yao: Conceptualization, Writing-review & editing. Chunyan Shui & Teng Li: Writing-review & editing. Sicheng Zhang& Hong Ma & Chao Li: Conceptualization, Funding, Writing-review & editing. All authors read and approved the final version of the manuscript.

Data availability
No datasets were generated or analysed during the current study.

Declarations

Ethics approval and consent to participate
Ethics Committee for Medical Research and New Medical Technology of Sichuan Cancer Hospital (SCCHEC-02–2024-109).

Competing interests
The authors declare no competing interests.

Author details
[1]Department of Oral and Maxillofacial Surgery, School of Stomatology, Guizhou Medical University, Guiyang 550004, China. [2]Department of Head and Neck Surgery, Sichuan Clinical Research Center for Cancer, Sichuan Cancer Hospital & Institute, Sichuan Cancer Center, University of Electronic Science and Technology of China, Chengdu 610041, China. [3]Department of Centre for Translational Research in Cancer, Radiation Oncology Key Laboratory of Sichuan Province, Sichuan Clinical Research Center for Cancer, Sichuan Cancer Center, University of Electronic Science and Technology of China, Chengdu 610041, China.

Received: 12 July 2024 Accepted: 27 December 2024
Published online: 26 February 2025

References

1. Sung H, Ferlay J, Siegel RL, et al. Global Cancer Statistics 2020: GLOBOCAN Estimates of Incidence and Mortality Worldwide for 36 Cancers in 185 Countries. CA Cancer J Clin. 2021;71(3):209–49.
2. Catalano MG, Poli R, Pugliese M, et al. Emerging molecular therapies of advanced thyroid cancer. Mol Aspects Med. 2010;31(2):215–26.
3. Fallahi P, Mazzi V, Vita R, et al. New therapies for dedifferentiated papillary thyroid cancer. Int J Mol Sci. 2015;16(3):6153–82.
4. Fagin JA, Wells SA, JR. Biologic and Clinical Perspectives on Thyroid Cancer. N Engl J Med. 2016;375(11):1054–67.
5. Xu J, Li Z, Su Q, et al. TRIM29 promotes progression of thyroid carcinoma via activating P13K/AKT signaling pathway. Oncol Rep. 2017;37(3):1555–64.
6. Hu J, Zhao N, Kong R, et al. Total thyroidectomy as primary surgical management for thyroid disease: surgical therapy experience from 5559 thyroidectomies in a less-developed region. World J Surg Oncol. 2016;14(1):20.
7. Pemayun TG. current diagnosis and management of thyroid nodules. Acta Med Indones. 2016;48(3):247–57.
8. Hu J, Yuan IJ, Mirshahidi S, et al. Thyroid Carcinoma: Phenotypic Features, Underlying Biology and Potential Relevance for Targeting Therapy. Int J Mol Sci. 2021;22(4):1950.
9. Puerto M, Borson-Chazot F, Tabarin A. Updates on therapy for medullary thyroid cancer in 2021. Ann Endocrinol (Paris). 2022;83(2):114–8.
10. Kim M, Kim BH. Current Guidelines for Management of Medullary Thyroid Carcinoma. Endocrinol Metab (Seoul). 2021;36(3):514–24.
11. Nozhat Z, Hedayati M. Medullary thyroid carcinoma: a review on ethical considerations in treatment of children. J Pediatr Endocrinol Metab. 2016;29(6):633–9.
12. Angelousi A, Hayes AR, Chatzellis E, et al. Metastatic medullary thyroid carcinoma: a new way forward. Endocr Relat Cancer. 2022;29(7):R85-r103.
13. Lin B, Ma H, Ma M, et al. The incidence and survival analysis for anaplastic thyroid cancer: a SEER database analysis. Am J Transl Res. 2019;11(9):5888–96.
14. Are C, Shaha AR. Anaplastic thyroid carcinoma: biology, pathogenesis, prognostic factors, and treatment approaches. Ann Surg Oncol. 2006;13(4):453–64.
15. Smallridge RC, Ain KB, Asa SL, et al. American Thyroid Association guidelines for management of patients with anaplastic thyroid cancer. Thyroid. 2012;22(11):1104–39.
16. Hong M, Wang N, Tan HY, et al. MicroRNAs and Chinese medicinal herbs: new possibilities in cancer therapy. Cancers (Basel). 2015;7(3):1643–57.
17. Luo Y, Feng Y, Song L, et al. A network pharmacology-based study on the anti-hepatoma effect of Radix Salviae Miltiorrhizae. Chin Med. 2019;14:27.
18. Chen Z, Zhang D, Yan S, et al. SAR study of Celastrol analogs targeting Nur77-mediated inflammatory pathway. Eur J Med Chem. 2019;177:171–87.
19. Luo D, Guo Y, Cheng Y, et al. Natural product Celastrol suppressed macrophage M1 polarization against inflammation in diet-induced obese mice via regulating Nrf2/HO-1 MAP kinase and NF-κB pathways. Aging (Albany NY). 2017;9(10):2069–82.
20. Lin FZ, Wang SC, Hsi YT, et al. Celastrol induces vincristine multidrug resistance oral cancer cell apoptosis by targeting JNK1/2 signaling pathway. Phytomedicine. 2019;54:1–8.
21. Liu X, Zhao P, Wang X, et al. Celastrol mediates autophagy and apoptosis via the ROS/JNK and Akt/mTOR signaling pathways in glioma cells. J Exp Clin Cancer Res. 2019;38(1):184.
22. Wagh PR, Desai P, Prabhu S, et al. Nanotechnology-Based Celastrol Formulations and Their Therapeutic Applications. Front Pharmacol. 2021;12:673209.
23. Accardo G, Conzo G, Esposito D, et al. Genetics of medullary thyroid cancer: An overview. Int J Surg. 2017;41(Suppl 1):S2-s6.
24. Santoro M, Carlomagno F. Central role of RET in thyroid cancer. Cold Spring Harb Perspect Biol. 2013;5(12):a009233.
25. Subbiah V, Shen T, Terzyan SS, et al. Structural basis of acquired resistance to selpercatinib and pralsetinib mediated by non-gatekeeper RET mutations. Ann Oncol. 2021;32(2):261–8.
26. Maniakas A, Zafereo M, Cabanillas ME. Anaplastic Thyroid Cancer: New Horizons and Challenges. Endocrinol Metab Clin North Am. 2022;51(2):391–401.
27. Xu H, Zhao H, Ding C, et al. Celastrol suppresses colorectal cancer via covalent targeting peroxiredoxin 1 [J]. Signal Transduct Target Ther. 2023;8(1):51.
28. Ye Y, Aihui Z, Anmao LI. Celastrol promotes apoptotic cell death in children neuroblastoma cells through caspases dependent pathway. J Tradit Chin Med. 2022;42(6):877–84.
29. Zhao Z, Wang Y, Gong Y, et al. Celastrol elicits antitumor effects by inhibiting the STAT3 pathway through ROS accumulation in non-small cell lung cancer. J Transl Med. 2022;20(1):525.

Publisher's Note